

# Greenberger-Horne-Zeilinger-type and $W$ -type entangled coherent states: Generation and Bell-type inequality tests without photon counting

Hyunseok Jeong<sup>1</sup> and Nguyen Ba An<sup>2,3</sup><sup>1</sup>*Centre for Quantum Computer Technology, Department of Physics, University of Queensland, Brisbane Qld 4072, Australia*<sup>2</sup>*Institute of Physics and Electronics, 10 Dao Tan, Thu Le, Ba Dinh, Hanoi, Vietnam*<sup>3</sup>*School of Computational Sciences, Korea Institute for Advanced Study, 207-43 Cheongryangni 2-dong, Dongdaemun-gu, Seoul 130-722, Korea*

(Received 16 November 2005; published 17 August 2006)

We study Greenberger-Horne-Zeilinger-type (GHZ-type) and  $W$ -type three-mode entangled coherent states. Both types of entangled coherent states violate Mermin's version of the Bell inequality with threshold photon detection (i.e., without photon counting). Such an experiment can be performed using linear optics elements and threshold detectors with significant Bell violations for GHZ-type entangled coherent states. However, to demonstrate Bell-type inequality violations for  $W$ -type entangled coherent states, additional nonlinear interactions are needed. We also propose an optical scheme to generate  $W$ -type entangled coherent states in free-traveling optical fields. The required resources for the generation are a single-photon source, a coherent state source, beam splitters, phase shifters, photodetectors, and Kerr nonlinearities. Our scheme does not necessarily require strong Kerr nonlinear interactions; i.e., weak nonlinearities can be used for the generation of the  $W$ -type entangled coherent states. Furthermore, it is also robust against inefficiencies of the single-photon source and the photon detectors.

DOI: [10.1103/PhysRevA.74.022104](https://doi.org/10.1103/PhysRevA.74.022104)

PACS number(s): 03.65.Ud, 03.67.Mn, 42.50.Dv, 42.50.-p

## I. INTRODUCTION

Quantum entanglement is a resource for quantum information processing and quantum computing. A large class of entangled states violate Bell-type inequalities [1–3], which means that the existence of such states cannot be explained by any local theory. It has been known that there exist at least two different types of multipartite entanglement: namely, the Greenberger-Horne-Zeilinger-type (GHZ-type) [4] entanglement and the  $W$ -type entanglement [5]. These two different types of entanglement are not equivalent and cannot be converted to each other by local unitary operations combined with classical communication [5].

Recently, entangled coherent states (ECS's) [6] in free-traveling optical fields have been found useful to perform tasks such as quantum teleportation [7,8], quantum computation [9–11], entanglement purification [12], quantum error corrections [13], etc. Most of these schemes use single-mode coherent-state superpositions (CSS's) as qubits and two-mode ECS's as quantum channels. Recently, Nguyen studied an optimal quantum information processing via multimode  $W$ -type ECS's [8]. In particular, it was shown that there exists a quantum information protocol which can be done only with  $W$ -type ECS's while GHZ-type ECS's fail to accomplish such a task [8]. As an example, remote symmetric entangling, which allows two distant parties to share a symmetric entangled state, strictly requires  $W$ -type three-mode ECS's. Even though there have been a number of studies of ECS's revealing their quantum nonlocality [14–17] and usefulness for quantum information processing [7–13], most of them have focused on two-mode ECS's while the characteristics of multimode ECS's, particularly the  $W$ -type ECS's, have been relatively less known.

A GHZ-type ECS can be generated using beam splitters with a single-mode CSS. Recently, there have been remark-

able theoretical suggestions which are within the reach of current technology [18–25] and an experimental attempt [26] for the generation of single-mode CSS's in free-traveling optical fields. However, the generation of  $W$ -type ECS's in free-traveling optical fields is not straightforward from single-mode CSS's. Very recently, Yuan *et al.* suggested a scheme to generate GHZ-type and  $W$ -type ECS's in cavity fields [27]. However, it should be noted that for most of tasks for quantum information processing [7–17], one needs to generate such ECS's *in free-traveling optical fields*.

In this paper, we suggest a scheme to generate  $W$ -type ECS's in free-traveling optical fields and study violations of the Mermin's version [28] of the Bell inequality [1] for both GHZ-type and  $W$ -type ECS's. Our study is closely associated with currently feasible experimental elements in quantum optics. The Bell's inequality test can be performed using linear optics elements and threshold detectors with large violations for GHZ-type ECS's but it requires additional nonlinear elements for  $W$ -type ECS's. As for our generation scheme of  $W$ -type ECS's, it requires a single-photon source, a coherent state source, beam splitters, phase shifters, and threshold photodetectors as well as weak nonlinearities. Our generation scheme is robust against inefficiencies of the single-photon source and the photodetectors.

We organize our paper as follows. In Sec. II we first outline possible schemes to generate multimode GHZ-type ECS's and then test the Bell-Mermin inequality for the three-mode case using photon parity (Sec. II A) and photon threshold (Sec. II B) measurements. Section III also has two subsections. Section III A presents a mechanism of generation of three-mode  $W$ -type ECS whose violation of the Bell-Mermin inequality is examined in Sec. III B by means of photon threshold measurements. Finally, we conclude in Sec. IV.

## II. GHZ-TYPE ENTANGLED COHERENT STATES

An  $N$ -mode GHZ-type ECS is defined as

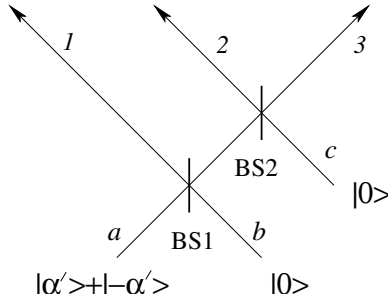


FIG. 1. An example of the generation of a GHZ-type three-mode ECS in free-traveling fields from a CSS using two beam splitters, BS1 with  $r_1=1/\sqrt{3}$  and BS2 with  $r_2=1/\sqrt{2}$ , where  $r_1$  and  $r_2$  are reflectivities of the beam splitters. Note that  $\alpha'=\sqrt{3}\alpha$ .

$$|\text{GHZ}, \alpha\rangle = c_1|\alpha, \alpha, \dots, \alpha\rangle_{1, \dots, N} + c_2|-\alpha, -\alpha, \dots, -\alpha\rangle_{1, \dots, N}, \quad (1)$$

where  $|\alpha, \alpha, \dots, \alpha\rangle_{1, \dots, N} = |\alpha\rangle_1 |\alpha\rangle_2 \cdots |\alpha\rangle_N$  with  $|\alpha\rangle_i$  a coherent state of amplitude  $\alpha$  while the complex coefficients  $c_1$  and  $c_2$  should satisfy the normalization condition. Such an entangled state can be generated with a single-mode CSS

$$|\text{CSS}\rangle = c_1|\alpha\rangle + c_2|-\alpha\rangle \quad (2)$$

and beam splitters. Recently, several feasible suggestions have been made for the generation of CSS's in free-traveling optical fields [18–25]. For example, it was found that simply squeezing a single photon results in a very good approximation of a single-mode CSS with amplitude  $\alpha \leq 1.2$  [21]. It was also pointed out that a weak Kerr nonlinearity can be useful to generate CSS's even under realistic decoherence [24]. The beam splitter operator  $\hat{B}(r, \phi)$  acting on two arbitrary modes  $a$  and  $b$  is represented as

$$\hat{B}(r, \phi) = \exp\left\{\frac{\theta}{2}(e^{i\phi}\hat{a}^\dagger\hat{b} - e^{-i\phi}\hat{b}^\dagger\hat{a})\right\}, \quad (3)$$

where the reflectivity  $r$  and transmittivity  $t$  are determined by  $\theta$  as

$$r = \sin \frac{\theta}{2}, \quad t = \cos \frac{\theta}{2}, \quad (4)$$

and  $\phi$  specifies the phase difference between the reflected and transmitted fields. We assume  $\phi = \pi$  throughout this paper. In particular, if a three-mode GHZ-type ECS of the form (1), where  $c_1 = -c_2$ , needs to be generated, one can pass the CSS,  $|\sqrt{3}\alpha\rangle - |-\sqrt{3}\alpha\rangle$  (unnormalized), through two beam splitters BS1 with  $r_1=1/\sqrt{3}$  and BS2 with  $r_2=1/\sqrt{2}$  successively as shown in Fig. 1. In general, to generate a GHZ-type ECS with an arbitrary mode number  $N$ , one should pass a CSS of the form  $|\sqrt{N}\alpha\rangle \pm |-\sqrt{N}\alpha\rangle$  through a sequence of  $N-1$  beam splitters with  $r_1=1/\sqrt{N}$ ,  $r_2=1/\sqrt{N-1}$ , ..., and  $r_{N-1}=1/\sqrt{2}$  or one can exploit a ‘‘tree scheme’’ that uses only 50:50 beam splitters combined, if necessary, with state-parity measurements (see, e.g., Ref. [29]).

### A. Bell-inequality violations of GHZ-type ECS's using photon-parity measurements

We now study the Bell-Mermin inequality for a three-mode GHZ-type ECS. Bell-inequality violations for two-mode ECS's have been studied with photon-parity and photon-threshold measurements [16,17]. We first study the Bell-Mermin inequality based upon the parity measurement and the displacement operation [30]. For that purpose we define an observable  $\Pi(\beta)$  as

$$\Pi(\beta) = D(\beta) \sum_{n=0}^{\infty} (|2n\rangle\langle 2n| - |2n+1\rangle\langle 2n+1|) D^\dagger(\beta), \quad (5)$$

where  $D(\beta)$  is the displacement operator,  $D(\beta) = \exp[\beta\hat{a}^\dagger - \beta^*\hat{a}]$ , for bosonic operators  $\hat{a}$  and  $\hat{a}^\dagger$ . Note that the eigenvalue of the observable  $\Pi(\beta)$  is 1 when an even number of photons is detected and it is  $-1$  when an odd number of photons is detected. The Bell-Mermin inequality [1,28] based on the observable  $\Pi(\beta)$  is

$$\begin{aligned} \text{BM}_\Pi = & |\langle \Pi(\beta_1)\Pi(\beta_2)\Pi(\beta_3) \rangle - \langle \Pi(\beta_1)\Pi(\beta'_2)\Pi(\beta'_3) \rangle \\ & - \langle \Pi(\beta'_1)\Pi(\beta_2)\Pi(\beta'_3) \rangle - \langle \Pi(\beta'_1)\Pi(\beta'_2)\Pi(\beta_3) \rangle| \leq 2, \end{aligned} \quad (6)$$

where  $\Pi(\beta_1)\Pi(\beta_2)\Pi(\beta_3) = \Pi_1(\beta_1) \otimes \Pi_2(\beta_2) \otimes \Pi_3(\beta_3)$  and we shall call  $\text{BM}_\Pi$  the Bell-Mermin function. The average value  $\langle \Pi(\beta_1)\Pi(\beta_2)\Pi(\beta_3) \rangle$  can be calculated using the identity

$$\langle \Pi(\beta_1)\Pi(\beta_2)\Pi(\beta_3) \rangle = \frac{\pi^3}{8} W(\beta_1, \beta_2, \beta_3), \quad (7)$$

where  $W(\beta_1, \beta_2, \beta_3)$  represents the Wigner function of the state of interest. The Wigner function of the three-mode GHZ-type ECS in Eq. (1), for the case of  $c_1 = \pm c_2$ , can be calculated as follows [31]. First, the characteristic function  $\chi_\pm(\eta_1, \eta_2, \eta_3)$  can be obtained as

$$\chi_\pm(\eta_1, \eta_2, \eta_3) = \text{Tr}[\rho_{\text{GHZ}} D(\eta_1) D(\eta_2) D(\eta_3)], \quad (8)$$

where  $\rho_{\text{GHZ}} = |\text{GHZ}, \alpha\rangle\langle \text{GHZ}, \alpha|$  and  $D(\eta_1)D(\eta_2)D(\eta_3) \equiv D_1(\eta_1) \otimes D_2(\eta_2) \otimes D_3(\eta_3)$ . The subscript plus (minus) sign of the characteristic function in Eq. (8) denotes  $c_1 = +c_2$  ( $c_1 = -c_2$ ). The characteristic function is then

$$\begin{aligned} \chi_\pm(\eta_1, \eta_2, \eta_3) = & \langle \text{GHZ}, \alpha | D(\eta_1) D(\eta_2) D(\eta_3) | \text{GHZ}, \alpha \rangle \\ = & M_\pm e^{-|\eta_1|^2/2 - |\eta_2|^2/2 - |\eta_3|^2/2} (\exp[\eta_1\alpha^* - \eta_1^*\alpha \\ & + \eta_2\alpha^* - \eta_2^*\alpha + \eta_3\alpha^* - \eta_3^*\alpha] + \exp[-\eta_1\alpha^* \\ & + \eta_1^*\alpha - \eta_2\alpha^* + \eta_2^*\alpha - \eta_3\alpha^* + \eta_3^*\alpha] \\ & \pm \exp[-6|\alpha|^2 - \eta_1\alpha^* - \eta_1^*\alpha - \eta_2\alpha^* - \eta_2^*\alpha \\ & - \eta_3\alpha^* - \eta_3^*\alpha] \pm \exp[-6|\alpha|^2 + \eta_1\alpha^* + \eta_1^*\alpha \\ & + \eta_2\alpha^* + \eta_2^*\alpha + \eta_3\alpha^* + \eta_3^*\alpha]), \end{aligned} \quad (9)$$

where  $M_\pm = 1/(2 \pm 2e^{-6|\alpha|^2})$ . The three-mode Wigner function is obtained from the characteristic function as

$$W_{\pm}(\beta_1, \beta_2, \beta_3) = \frac{1}{\pi^6} \int d^2 \eta_1 d^2 \eta_2 d^2 \eta_3 \exp[\eta_1^* \beta_1 - \eta_1 \beta_1^* + \eta_2^* \beta_2 - \eta_2 \beta_2^* + \eta_3^* \beta_3 - \eta_3 \beta_3^*] \chi_{\pm}(\eta_1, \eta_2, \eta_3). \quad (10)$$

After the integration, the Wigner function of the GHZ-type ECS is

$$W_{\pm}(\beta_1, \beta_2, \beta_3) = N_{\pm} (\exp[-2|\beta_1 - \alpha|^2 - 2|\beta_2 - \alpha|^2 - 2|\beta_3 - \alpha|^2] + \exp[-2|\beta_1 + \alpha|^2 - 2|\beta_2 + \alpha|^2 - 2|\beta_3 + \alpha|^2] \pm e^{-6|\alpha|^2} \{ \exp[-2(\beta_1 - \alpha)(\beta_1 + \alpha)^* - 2(\beta_2 - \alpha)(\beta_2 + \alpha)^* - 2(\beta_3 - \alpha)(\beta_3 + \alpha)^*] + \exp[-2(\beta_1 - \alpha)^*(\beta_1 + \alpha) - 2(\beta_2 - \alpha)^*(\beta_2 + \alpha) - 2(\beta_3 - \alpha)^*(\beta_3 + \alpha)] \}), \quad (11)$$

with  $N_{\pm} = 8 / [\pi^3 (2 \pm 2e^{-6|\alpha|^2})]$ . The Bell-Mermin function  $BM_{\Pi}$  has 12 variables, and it is highly nontrivial to find the global maximum values of  $BM_{\Pi}$  for all 12 variables. Fortunately, some local maximum values which violate the Bell-Mermin inequality can be found numerically using the method of steepest descent [32], which has been plotted in Fig. 2.

Figure 2 shows that as  $\alpha$  increases the value  $BM_{\Pi}$  of the Bell-violation first grows and then asymptotically approaches the value of 3.6 when  $\alpha \rightarrow \infty$  for the GHZ-type ECS's of  $c_1 = c_2$  and  $c_1 = -c_2$ . For instance, when  $\alpha = 10$ , the Bell-Mermin function is found to be  $BM_{\Pi} \approx 3.58$  at  $\text{Re}[\beta_1] = \text{Re}[\beta_2] = \text{Im}[\beta_3] = \text{Re}[\beta'_1] = \text{Re}[\beta'_2] = \text{Re}[\beta'_3] = 0$ ,  $\text{Im}[\beta_1] = -\text{Im}[\beta'_1] = -0.020$ ,  $\text{Im}[\beta_2] = -\text{Re}[\beta_3] = -0.0519$ , and  $\text{Im}[\beta'_2] = -\text{Re}[\beta'_3] = -0.0259$  for both cases of  $c_1 = c_2$  and  $c_1 = -c_2$ . It is interesting to note that even when  $\alpha$  is extremely small, the GHZ-type ECS of  $c_1 = -c_2$  [dashed curve in Fig. 2(b)] still violates the Bell-Mermin inequality whereas the GHZ-type ECS of  $c_1 = c_2$  does not [solid curve in Fig. 2(b)]. This is due to the singular behavior of the GHZ-type ECS of  $c_1 = -c_2$  when  $\alpha$  approaches zero. When  $\alpha$  approaches zero, the GHZ-type ECS becomes a vacuum product state without entanglement—i.e.,  $|0\rangle|0\rangle|0\rangle$ —unless  $c_1 = -c_2$ . However, if  $c_1 = -c_2$ , as  $\alpha$  approaches zero, the GHZ-type ECS generated using beam splitters as shown in Fig. 1 will approach

$$\frac{1}{\sqrt{3}} (|1\rangle|0\rangle|0\rangle + |0\rangle|1\rangle|0\rangle + |0\rangle|0\rangle|1\rangle), \quad (12)$$

which is a highly nonlocal entangled state. This can be understood as follows. In order to generate the GHZ-type ECS of  $c_1 = -c_2$  using two beam splitters BS1 and BS2 as sketched in Fig. 1, a CSS of  $c_1 = -c_2$  is needed. The CSS of  $c_1 = -c_2$  approaches the single-photon state  $|1\rangle$  for  $\alpha \rightarrow 0$  [17]. This single-photon state after passing through BS1 and BS2 in Fig. 1 results in the state given by Eq. (12). Therefore, one can expect that the GHZ-type ECS approaches the state (12) showing Bell-type-inequality violations only when  $c_1 = -c_2$ . Such a singular behavior is in agreement with the previous studies for two-mode ECS's [16,17]. Namely, a two-mode

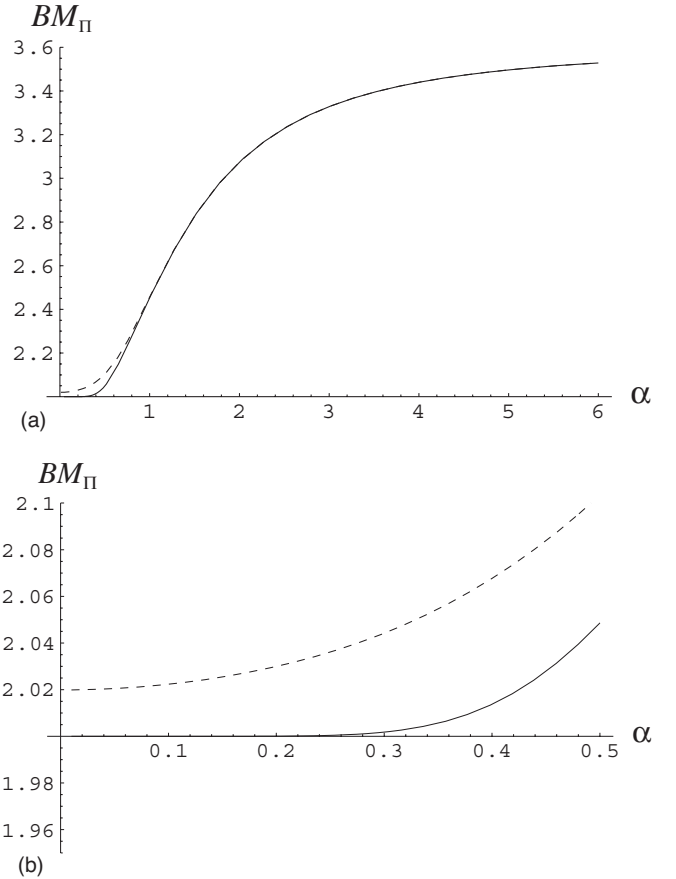


FIG. 2. Violations of the Bell-Mermin inequality for the GHZ-type ECS of amplitude  $\alpha$  using parity measurements.  $BM_{\Pi}$  represents the Bell-Mermin function defined in the text which is supposed to be not greater than 2 by a local hidden-variable theory. (a) As  $\alpha$  increases the violation increases and saturates at  $\approx 3.6$  for the GHZ-type ECS's of  $c_1 = c_2$  (solid line) and  $c_1 = -c_2$  (dashed line). (b) Even when  $\alpha$  is extremely small the GHZ-type ECS of  $c_1 = -c_2$  (dashed line) still violates the Bell-Mermin inequality while the GHZ-type ECS of  $c_1 = c_2$  does not.

ECS  $|\alpha, \alpha\rangle - |-\alpha, -\alpha\rangle$  (unnormalized) violates the Bell inequality even in the limit  $\alpha \rightarrow 0$  because the two-mode ECS becomes a single-photon entangled state  $(|0, 1\rangle + |1, 0\rangle) / \sqrt{2}$ . Nevertheless, the two-mode ECS  $|\alpha, \alpha\rangle + |-\alpha, -\alpha\rangle$  (unnormalized) ceases to violate the Bell inequality in the limit  $\alpha \rightarrow 0$  as in this limit it becomes a vacuum product state  $|0\rangle|0\rangle$ .

The displacement operation used in this type of Bell-inequality tests can be effectively performed in an optics experiment by means of a beam splitter with the transmission coefficient close to unity and a strong coherent state being injected into the other input port [33]. However, the photon-parity measurements should distinguish between odd and even number of photons. This is extremely hard because the detectors which perfectly discriminate between neighboring photon numbers (i.e.,  $n$  and  $n+1$  photons) do not exist at the present status of technology. On the other hand, threshold photon detection, which discriminates between the presence and absence of photons, is available with a reasonably high probability using current technology [34]. Therefore, in what follows, we shall focus on the Bell-Mermin-inequality test

using only threshold photon detection and displacement operations.

### B. Bell-inequality violations of GHZ-type ECS's using photon-threshold measurements

We define an observable  $A(\beta)$  for a Bell-Mermin inequality test with the threshold photon measurements and the displacement operations as

$$A(\beta) = D(\beta)^\dagger \left( |0\rangle\langle 0| - \sum_{n=1}^{\infty} |n\rangle\langle n| \right) D(\beta), \quad (13)$$

whose eigenvalue is 1 when no photon are detected and  $-1$  when any  $n \geq 1$  photon(s) are detected. The Bell-Mermin inequality based on the observable  $A(\beta)$  reads

$$\begin{aligned} BM_A = & |\langle A(\beta_1)A(\beta_2)A(\beta_3) \rangle - \langle A(\beta_1)A(\beta'_2)A(\beta'_3) \rangle \\ & - \langle A(\beta'_1)A(\beta_2)A(\beta'_3) \rangle - \langle A(\beta'_1)A(\beta'_2)A(\beta_3) \rangle| \leq 2. \end{aligned} \quad (14)$$

In order to calculate  $BM_A$  for the ECS's, we first compute the following quantities:

$$J(\beta) \equiv \langle \alpha | A(\beta) | \alpha \rangle = 2 \exp[-|\alpha + \beta|^2] - 1, \quad (15)$$

$$K(\beta) \equiv \langle -\alpha | A(\beta) | -\alpha \rangle = 2 \exp[-|\alpha - \beta|^2] - 1, \quad (16)$$

$$\begin{aligned} L(\beta) & \equiv \langle \alpha | A(\beta) | -\alpha \rangle \\ & = \exp \left[ -\frac{1}{2}|\alpha + \beta|^2 - \frac{1}{2}|\alpha - \beta|^2 + \alpha\beta^* - \alpha^*\beta \right] \\ & \quad \times (2 - e^{-(\alpha + \beta)^*(\alpha - \beta)}), \end{aligned} \quad (17)$$

In terms of these quantities we have, for the GHZ-type three-mode ECS,

$$\begin{aligned} \langle A(\beta_1)A(\beta_2)A(\beta_3) \rangle & = |c_1|^2 J(\beta_1)J(\beta_2)J(\beta_3) \\ & \quad + |c_2|^2 K(\beta_1)K(\beta_2)K(\beta_3) \\ & \quad + 2\Re[c_1 c_2^* L(\beta_1)L(\beta_2)L(\beta_3)], \end{aligned} \quad (18)$$

from which one can calculate  $BM_A$  in Eq. (14). The value of this violation can be found numerically using again the method of steepest descent [32], which has been plotted for the GHZ-type ECS's of  $c_1 = -c_2$  in Fig. 3. As can be seen from the figure, the Bell-Mermin inequality is largely violated for a small  $\alpha$ . The maximum value is found to be  $BM_A \approx 2.5$  when  $\alpha \approx 0.18$  at  $\text{Re}[\beta_1] = \text{Re}[\beta_2] = \beta'_2 = \beta'_3 = 0$ ,  $\text{Im}[\beta_1] = \text{Im}[\beta_2] = -0.371$ ,  $\text{Re}[\beta_3] = \text{Im}[\beta_3] = -0.295$ , and  $\text{Re}[\beta'_1] = \text{Im}[\beta'_1] = 0.173$ . Even when  $\alpha$  is extremely small, the inequality is still significantly violated because we have considered the GHZ-type ECS of  $c_1 = -c_2$ . As explained in the previous subsection, the GHZ-type ECS with this particular relative phase approaches the single-photon entangled state (12) for  $\alpha \rightarrow 0$ . However, the Bell-Mermin inequality ceases to be violated when  $\alpha \geq 0.6$  as shown in Fig. 3. Comparing Figs. 2 and 3, we immediately learn that the photon-thresh-

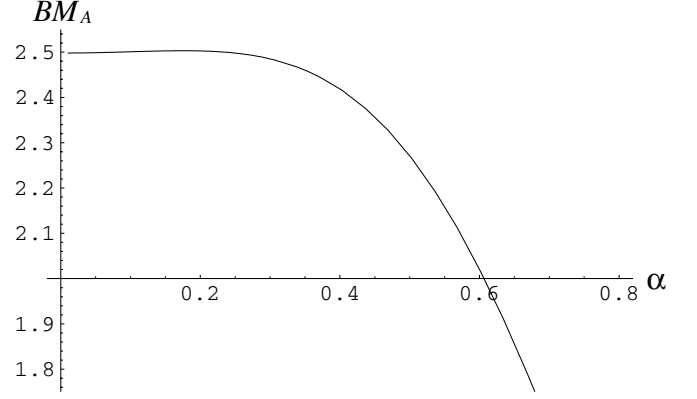


FIG. 3. Violations of Bell-Mermin inequality for a GHZ-type ECS of amplitude  $\alpha$  using threshold photodetectors.  $BM_A$  represents the Bell-Mermin function defined in the text, Eq. (14), which is supposed to be less than or equal to 2 by a local hidden-variable theory. As  $\alpha$  increases the violation first decreases and then ceases starting from  $\alpha \approx 0.6$ .

old measurements are more efficient to test the Bell-Mermin inequality for GHZ-type ECS's with small amplitudes, while the photon-parity measurements are more efficient for GHZ-type ECS's with large amplitudes.

This result is due to the characteristic of the observable  $A(\beta)$  in Eq. (13) composed of the photon-threshold measurement and the displacement operations. It should be noted that a Bell-type-inequality test depends not only on the state being considered but also on the type of the measurements and the type of the random rotations used for the test. A previous study [17] presents a similar result for nonclassical two-mode fields: two-mode ECS's and two-mode squeezed states significantly violate the Bell-Clauser-Horne inequality [3] using the photon-threshold detection and the displacement operations only when the coherent amplitudes (or the degree of squeezing) are small. All these results suggest that the photon-threshold measurements and the displacement operations are efficient for a Bell-type-inequality test for the continuous-variable states only when the average photon number of the states is appropriately small. In this connection, the photon-threshold measurements and the displacement operations prove to be very suitable as an efficient tool to test a Bell-type inequality in a quantum optics experiment because GHZ-type ECS's with small amplitudes are relatively easy to be generated from CSS's with small amplitudes [21,24].

## III. W-TYPE ENTANGLED COHERENT STATES

### A. Generation of W-type ECS's

A three-mode W-type ECS is [8]

$$\begin{aligned} |W, \alpha\rangle & = a_1 |\alpha, -\alpha, -\alpha\rangle_{123} + a_2 |-\alpha, \alpha, -\alpha\rangle_{123} \\ & \quad + a_3 |-\alpha, -\alpha, \alpha\rangle_{123}, \end{aligned} \quad (19)$$

where the coefficients should meet the normalization condition. Our W-type ECS generation scheme is depicted in Fig. 4. We will first describe how to generate a three-mode

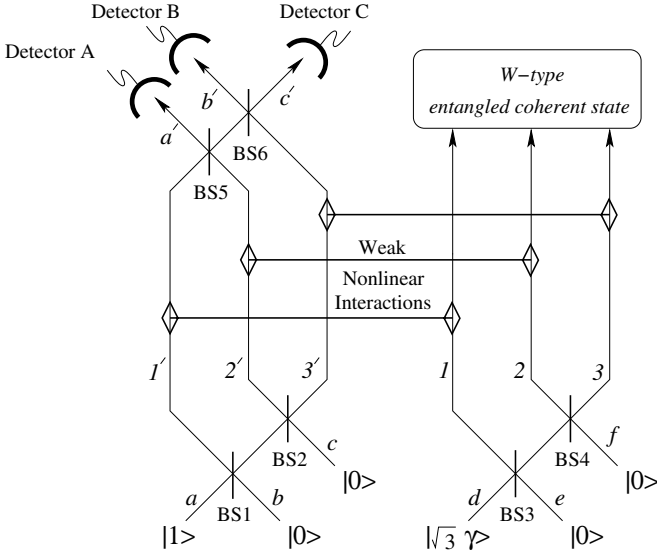


FIG. 4. A schematic of our scheme to generate a  $W$ -type ECS. A  $W$ -type ECS is generated when detector B or detector C clicks.

$W$ -type ECS with  $|a_1|=|a_2|=|a_3|$ . However, it can be simply generalized to the case with arbitrary coefficients. In Fig. 4, the reflectivity of the first beam splitter BS1 is  $r_1=\sqrt{2/5}$  and that of the second beam splitter BS2 is  $r_2=\sqrt{2/3}$ . Through BS1 and BS2, the initial state of the left part in Fig. 4 becomes

$$\hat{B}_{BS2}\hat{B}_{BS1}|1,0,0\rangle_{abc} = \frac{1}{\sqrt{5}}(\sqrt{2}|1,0,0\rangle + \sqrt{2}|0,1,0\rangle + |0,0,1\rangle)_{1'2'3'}. \quad (20)$$

In the right part of Fig. 4, three coherent states  $|\gamma\rangle_1|\gamma\rangle_2|\gamma\rangle_3$  are prepared using a coherent state  $|\sqrt{3}\gamma\rangle_d$  and two beam splitters BS3 and BS4 with reflectivities  $r_3=1/\sqrt{3}$  and  $r_4=1/\sqrt{2}$ , respectively. Then the cross Kerr nonlinear interactions are to be used between mode 1' (2', 3') and mode 1 (2, 3) as shown in Fig. 4. The interaction Hamiltonian of the cross Kerr nonlinear interaction between two arbitrary modes  $a$  and  $b$ ,  $H_{CK}=\hbar\chi a^\dagger ab^\dagger b$ , causes transformations  $|0\rangle_a|\gamma\rangle_b \rightarrow |0\rangle_a|\gamma\rangle_b$  and  $|1\rangle_a|\gamma\rangle_b \rightarrow |1\rangle_a|\gamma e^{i\theta}\rangle_b$ , where  $\theta=\chi t$  with  $\chi$  the coupling constant and  $t$  the interaction time. Even though available Kerr nonlinearities are extremely weak, very recently it has been discussed that use of strong coherent fields may circumvent this problem even under the realistic assumption of decoherence [24]. Therefore, in our scheme,  $\gamma$  is supposed to be large. The nonlinear interactions transform the total state to

$$\begin{aligned} & \frac{1}{\sqrt{5}}(\sqrt{2}|1,0,0\rangle_{1'2'3'}|\gamma e^{i\theta}, \gamma, \gamma\rangle_{123} \\ & + \sqrt{2}|0,1,0\rangle_{1'2'3'}|\gamma, \gamma e^{i\theta}, \gamma\rangle_{123} \\ & + |0,0,1\rangle_{1'2'3'}|\gamma, \gamma, \gamma e^{i\theta}\rangle_{123}). \end{aligned} \quad (21)$$

Then, two 50:50 beam splitters BS5 and BS6 are applied to modes 1', 2', and 3' as shown in Fig. 4. It is straightforward

to verify that the total state after passing through BS5 and BS6 becomes

$$\begin{aligned} & \frac{1}{\sqrt{5}}|1,0,0\rangle_{a'b'c'}(|\gamma e^{i\theta}, \gamma\rangle + |\gamma, \gamma e^{i\theta}\rangle)|\gamma\rangle_{123} + \frac{1}{\sqrt{10}}(|0,1,0\rangle \\ & + |0,0,1\rangle)_{a'b'c'}(|\gamma e^{i\theta}, \gamma, \gamma\rangle + |\gamma, \gamma e^{i\theta}, \gamma\rangle + |\gamma, \gamma, \gamma e^{i\theta}\rangle)_{123}. \end{aligned} \quad (22)$$

Now, detectors A, B, and C (see Fig. 4) are set to detect photons of modes  $a'$ ,  $b'$ , and  $c'$ , respectively. If detector A clicks, the resulting state (unnormalized) is reduced to

$$(|\gamma e^{i\theta}, \gamma\rangle + |\gamma, \gamma e^{i\theta}\rangle)_{12}|\gamma\rangle_3, \quad (23)$$

while either detector B or C clicks it is

$$(|\gamma e^{i\theta}, \gamma, \gamma\rangle + |\gamma, \gamma e^{i\theta}, \gamma\rangle + |\gamma, \gamma, \gamma e^{i\theta}\rangle)_{123}. \quad (24)$$

The final step is to apply the displacement operators  $D(x) \otimes D(x) \otimes D(x)$ , with  $x=-(\gamma+\gamma e^{i\theta})/2$ , on the state in (24). Such operations are to change the state in (24) to the symmetric form in the phase space in Eq. (19). As we have pointed out previously, the displacement operation can be effectively performed using a strong coherent fields (an additional local oscillator in this case) and a biased beam splitter. It can be shown that the final state after the displacement operations is

$$N_W(|\alpha, -\alpha, -\alpha\rangle + |-\alpha, \alpha, -\alpha\rangle + |-\alpha, -\alpha, \alpha\rangle)_{123}, \quad (25)$$

where  $\alpha=\gamma(e^{i\theta}-1)/2$  and  $N_W=1/\sqrt{3+6e^{-4|\alpha|^2}}$ . However, the final displacement operations are only local unitary transformations which cannot change the entanglement nature of a quantum state. Therefore, we stress that the generated state (24) is already a  $W$ -type entangled coherent state and the displacement operations mentioned above are just an optional step.

Note that the success probability of getting the  $W$ -type three-mode ECS, Eq. (25), is 3/5, while a two-mode ECS  $(|\alpha, -\alpha\rangle + |-\alpha, \alpha\rangle)_{12}$  (unnormalized) can be obtained with a probability of 2/5 from the state in Eq. (23) using similar displacement operations. Even though our case concerned  $a_1=a_2=a_3$ , arbitrary values of these coefficients can also be tailored by changing the reflectivities and phases of the beam splitters BS1 and BS2. For example, if one needs to generate a  $W$ -type ECS of  $a_1=a_2=-a_3$ , the phase of BS2,  $\phi_2$ , should be set to be  $\phi_2=\pi$ . It is worth emphasizing that our scheme depicted in Fig. 4 does not require highly efficient detectors because the inefficiency of the detectors does not affect the quality of the generated  $W$ -type ECS's, yet it might decrease the success probability to be lower than 3/5. Also of interest is the fact that generally not all the three detectors are necessary in our scheme. For example, only one of the detectors B and C (but not both of them) would suffice to generate a  $W$ -type ECS with a success probability of 3/10 when the detector clicks. Furthermore, our scheme is robust to inefficiencies of the single-photon source as well as of the photon detectors. The inefficiencies of the single-photon source and the photon detectors will only reduce the success probability but will not affect the quality of the  $W$ -type ECS's to be generated.

### B. Bell-inequality violations of $W$ -type ECS's using photon-threshold measurements

We now investigate the Bell-Mermin inequality for the  $W$ -type ECS's in Eq. (25). According to our numerical study, the Bell-Mermin inequality is not violated for  $W$ -type ECS's by the methods used for GHZ-type ECS's in this paper. In this case, the required random rotations for the Bell tests cannot be achieved by the displacement operation [35]. Therefore, in this subsection, we shall alternatively approach the problem by treating the coherent state  $|\alpha\rangle$  and the vacuum  $|0\rangle$  as a logical qubit basis  $\{|0_L\rangle, |1_L\rangle\}$ : namely,  $|0_L\rangle \equiv |0\rangle$  and  $|1_L\rangle \equiv |\alpha\rangle$ . Since our approach here becomes a closer analogy of the ideal qubit case for a  $W$ -type entangled state [36] when  $\alpha$  becomes large, it is expected that the Bell-Mermin inequality would strongly be violated in this large- $\alpha$  limit. The first step to make use of the logical qubits is to displace a  $W$ -type ECS of the form given by Eq. (25) to a  $W$ -type ECS of the following form:

$$|\Psi_w\rangle = \mathcal{N}_w(|\alpha, 0, 0\rangle + |0, \alpha, 0\rangle + |0, 0, \alpha\rangle), \quad (26)$$

where  $\mathcal{N}_w = 1/\sqrt{3+6e^{-|\alpha|^2}}$ . This transformation can be done by the local displacement operations  $D(\alpha') \otimes D(\alpha') \otimes D(\alpha')$  on a  $W$ -type ECS  $|W, \alpha'\rangle$  with  $a_1 = a_2 = a_3$ , where  $\alpha' = \alpha/2$ . One can directly transform the state (24) to the state (26) by appropriate displacement operations. Let us introduce a unitary transformation  $U_X$  for a coherent-state qubit:

$$U_X = D\left(\frac{\alpha}{2}\right) U_K(\pi/\chi) D\left(-\frac{\alpha}{2}\right), \quad (27)$$

where  $U_K(t) = e^{iH_K t/\hbar}$  and  $H_K = \hbar\chi(a^\dagger a)^2$  with  $t$  the interaction time in a single-mode Kerr nonlinear medium. In other words, besides the displacement operations, additional single-mode Kerr nonlinear interactions described by the interaction Hamiltonian  $H_K$  with the interaction time  $t = \pi/\chi$  need to be used for necessary random rotations of a Bell-type-inequality test. Even though such strong nonlinear interactions are very demanding in a real experiment, there was an experimental report for a successful measurement of giant Kerr nonlinearity [37]. Using the identity [38]  $U_K(\pi/\chi)|\alpha\rangle = e^{-i\pi/4}(|\alpha\rangle + i|-\alpha\rangle)/\sqrt{2}$ , one can easily verify

$$\begin{aligned} U_X|0\rangle &= \frac{e^{-i\pi/4}}{\sqrt{2}}(|0\rangle + i|\alpha\rangle), \\ U_X|\alpha\rangle &= \frac{e^{-i\pi/4}}{\sqrt{2}}(i|0\rangle + |\alpha\rangle), \end{aligned} \quad (28)$$

which corresponds to a  $-\pi/2$  rotation around the  $x$  axis up to the irrelevant global phase factor for the qubit basis  $\{|0\rangle, |\alpha\rangle\}$ . Because of the additional Kerr nonlinearities used, we define an observable  $\mathcal{A}(\tau)$ , which is slightly different from  $A(\beta)$  in Eq. (13):

$$\mathcal{A}(\tau) = U(\tau)^\dagger \left( |0\rangle\langle 0| - \sum_{n=1}^{\infty} |n\rangle\langle n| \right) U(\tau), \quad (29)$$

where  $\tau$  is either 0 or 1 and

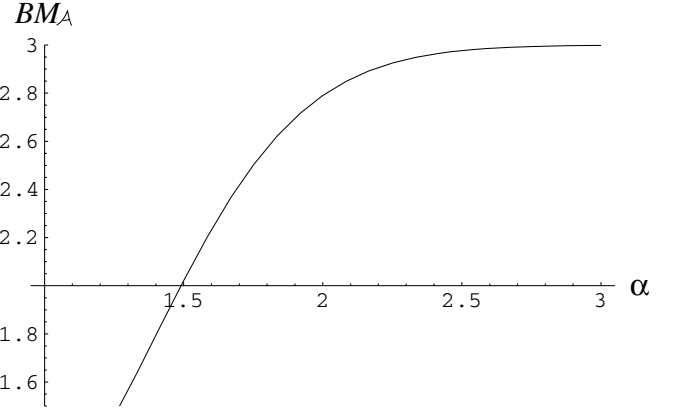


FIG. 5. Violations of the Bell-Mermin inequality for a  $W$ -type ECS of amplitude  $\alpha$  using threshold photodetectors and nonlinear interactions. The Bell-Mermin function  $BM_A$  is larger than the classical bound 2 for  $\alpha \gtrsim 1.49$ .

$$U(0) = 1, \quad U(1) = U_X. \quad (30)$$

When  $\alpha$  is large, the states  $|0\rangle$  and  $|\alpha\rangle$  are eigenstates of the observable  $\mathcal{A}(0)$  with the eigenvalues 1 and  $-1$ , respectively. The Bell-Mermin inequality is then constructed as

$$\begin{aligned} BM_A &= |\langle \mathcal{A}(\tau_1)\mathcal{A}(\tau_2)\mathcal{A}(\tau_3) \rangle - \langle \mathcal{A}(\tau_1)\mathcal{A}(\tau'_2)\mathcal{A}(\tau'_3) \rangle \\ &\quad - \langle \mathcal{A}(\tau'_1)\mathcal{A}(\tau_2)\mathcal{A}(\tau'_3) \rangle - \langle \mathcal{A}(\tau'_1)\mathcal{A}(\tau'_2)\mathcal{A}(\tau_3) \rangle| \leq 2. \end{aligned} \quad (31)$$

Taking  $\tau_1 = \tau_2 = \tau_3 = 0$  and  $\tau'_1 = \tau'_2 = \tau'_3 = 1$  and using Eqs. (26)–(30), it is straightforward to calculate

$$\langle \mathcal{A}(0)\mathcal{A}(0)\mathcal{A}(0) \rangle = \frac{4 - e^{\alpha^2}}{2 + e^{\alpha^2}} \equiv \mathcal{V}(\alpha) \quad (32)$$

and

$$\begin{aligned} \langle \mathcal{A}(0)\mathcal{A}(1)\mathcal{A}(1) \rangle &= \langle \mathcal{A}(1)\mathcal{A}(0)\mathcal{A}(1) \rangle = \langle \mathcal{A}(1)\mathcal{A}(1)\mathcal{A}(0) \rangle \\ &= -\frac{2 - 2e^{-2\alpha^2} - 7e^{-\alpha^2} - 2e^{\alpha^2}}{3(2 + e^{\alpha^2})} \equiv \mathcal{W}(\alpha), \end{aligned} \quad (33)$$

where  $\alpha$  was assumed to be real. Then the Bell-Mermin function is obtained as

$$BM_A = |\mathcal{V}(\alpha) - 3\mathcal{W}(\alpha)| = \left| \frac{6 - 2e^{-2\alpha^2} - 7e^{-\alpha^2} - 3e^{\alpha^2}}{2 + e^{\alpha^2}} \right|. \quad (34)$$

The Bell-Mermin function  $BM_A$  is plotted in Fig. 5. The Bell-Mermin inequality begins to be violated from  $\alpha \approx 1.49$ , and the value of  $BM_A$  rapidly saturates to 3 as  $\alpha$  grows.

## IV. CONCLUSION

We have studied Mermin's version of the Bell inequality for GHZ-type and  $W$ -type three-mode ECS's. Both types of ECS's violate the Bell-Mermin inequality with threshold

photon detection (i.e., without photon counting). Such an experiment can be performed using linear optics elements and threshold detectors with large violations for GHZ-type ECS's. However, it would be experimentally more difficult to demonstrate Bell-type inequality violations for *W*-type ECS's since it requires additional strong nonlinear interactions. We have found out that the photon-threshold measurements are more efficient to test the Bell-Mermin inequality for the GHZ-type ECS's of small amplitudes, but for the *W*-type ECS's of large amplitudes: an interesting fact that reflects a clear inequivalence between the two types of ECS's. The generation of a GHZ-type ECS requires a CSS and two beam splitters. Recently, there was an experimental report to generate a CSS in a real laboratory even though the fidelity was limited [26]. Based on the recent theoretical [18–25] and experimental [26] progress, it is expected that the realization of a CSS with higher fidelity can be achieved in the foreseeable future.

We have also proposed a scheme to generate *W*-type ECS's for three free-traveling optical fields (generalization to more than three fields is possible). The required resources are a single-photon source, a coherent state source, beam splitters, phase shifters, photodetectors, and Kerr nonlinearities. Our scheme does not necessarily require strong Kerr nonlinear interactions; i.e., weak nonlinearities can be useful for

our scheme. Furthermore, it is also robust against inefficiencies of the single-photon source and the photon detectors.

It should be noted that good mode matching would be required at BS5 and BS6 in Fig. 4, while efficient mode matching between optical fields at a beam splitter is being performed in a real laboratory condition using present technology [39]. The dark count rate of photodetectors will affect the fidelity of the generated *W*-type ECS's. Currently, highly efficient detectors have relatively high dark count rates while less efficient detectors have very low dark count rates [34]. We emphasize that our scheme here does not require highly efficient detectors. Compared with the scheme to generate a CSS with only one weak nonlinear interaction [24], from which the generation of GHZ-type ECS's can be straightforwardly performed, the most demanding element in our scheme would be to control the three weak nonlinear interactions in Fig. 4. However, such techniques using weak nonlinearities are being intensively studied [24,25,40,41].

#### ACKNOWLEDGMENTS

H.J. is supported by the Australian Research Council and N.B.A. by the Vietnam Institute of Physics and Electronics and Korea Institute for Advanced Study.

- 
- [1] S. Bell, *Physics* (Long Island City, N.Y.) **1**, 195 (1964).
  - [2] J. F. Clauser, M. A. Horne, A. Shimony, and R. A. Holt, *Phys. Rev. Lett.* **23**, 880 (1969).
  - [3] J. F. Clauser and M. A. Horne, *Phys. Rev. D* **10**, 526 (1974).
  - [4] D. M. Greenberger, M. A. Horne, and A. Zeilinger, in *Bell's Theorem, Quantum Theory, and Conceptions of the Universe*, edited by M. Kafatos (Kluwer, Dordrecht, 1989), p. 69.
  - [5] W. Dür, G. Vidal, and J. I. Cirac, *Phys. Rev. A* **62**, 062314 (2000).
  - [6] B. C. Sanders, *Phys. Rev. A* **45**, 6811 (1992).
  - [7] S. J. van Enk and O. Hirota, *Phys. Rev. A* **64**, 022313 (2001); H. Jeong, M. S. Kim, and J. Lee, *ibid.* **64**, 052308 (2001); X. Wang, *ibid.* **64**, 022302 (2001); Nguyen Ba An, *ibid.* **68**, 022321 (2003).
  - [8] Nguyen Ba An, *Phys. Rev. A* **69**, 022315 (2004).
  - [9] H. Jeong and M. S. Kim, *Phys. Rev. A* **65**, 042305 (2002).
  - [10] T. C. Ralph, W. J. Munro, and G. J. Milburn, *Proc. SPIE* **4917**, 1 (2002).
  - [11] T. C. Ralph, A. Gilchrist, G. J. Milburn, W. J. Munro, and S. Glancy, *Phys. Rev. A* **68**, 042319 (2003).
  - [12] H. Jeong and M. S. Kim, *Quantum Inf. Comput.* **2**, 208 (2002); J. Clausen, L. Knöll, and D.-G. Welsch, *Phys. Rev. A* **66**, 062303 (2002).
  - [13] P. T. Cochrane, G. J. Milburn, and W. J. Munro, *Phys. Rev. A* **59**, 2631 (1999); S. Glancy, H. M. Vasconcelos, and T. C. Ralph, *ibid.* **70**, 022317 (2004).
  - [14] A. Mann, B. C. Sanders, and W. J. Munro, *Phys. Rev. A* **51**, 989 (1995).
  - [15] J. Wenger, M. Hafezi, F. Grosshans, R. Tualle-Brouiri, and P. Grangier, *Phys. Rev. A* **67**, 012105 (2003).
  - [16] D. Wilson, H. Jeong, and M. S. Kim, *J. Mod. Opt.* **49**, 851 (2002).
  - [17] H. Jeong, W. Son, M. S. Kim, D. Ahn, and C. Brukner, *Phys. Rev. A* **67**, 012106 (2003).
  - [18] F. De Martini, *Phys. Rev. Lett.* **81**, 2842 (1998); F. De Martini, M. Fortunato, P. Tombesi, and D. Vitali, *Phys. Rev. A* **60**, 1636 (1999).
  - [19] M. Dakna, J. Clausen, L. Knöll, and D.-G. Welsch, *Phys. Rev. A* **59**, 1658 (1999); J. Clausen, M. Dakna, L. Knöll, and D.-G. Welsch, *Opt. Commun.* **179**, 189 (2000).
  - [20] M. Paternostro, M. S. Kim, and B. S. Ham, *Phys. Rev. A* **67**, 023811 (2003); M. Paternostro, M. S. Kim, and B. S. Ham, *J. Mod. Opt.* **50**, 2565 (2003).
  - [21] A. P. Lund, H. Jeong, T. C. Ralph, and M. S. Kim, *Phys. Rev. A* **70**, 020101(R) (2004); H. Jeong, A. P. Lund, and T. C. Ralph, *ibid.* **72**, 013801 (2005).
  - [22] H. Jeong, M. S. Kim, T. C. Ralph, and B. S. Ham, *Phys. Rev. A* **70**, 061801(R) (2004).
  - [23] B. Wang and L.-M. Duan, *Phys. Rev. A* **72**, 022320 (2005).
  - [24] H. Jeong, *Phys. Rev. A* **72**, 034305 (2005).
  - [25] M. S. Kim and M. Paternostro, e-print quant-ph/0510057.
  - [26] J. Wenger, R. Tualle-Brouiri, and P. Grangier, *Phys. Rev. Lett.* **92**, 153601 (2004).
  - [27] C.-H. Yuan, Y.-C. Ou, and Z.-M. Zhang, e-print quant-ph/0509069.
  - [28] N. D. Mermin, *Phys. Rev. Lett.* **65**, 1838 (1990).
  - [29] Nguyen Ba An and J. Kim, e-print quant-ph/0303149.
  - [30] K. Banaszek and K. Wódkiewicz, *Phys. Rev. A* **58**, 4345 (1998); *Phys. Rev. Lett.* **82**, 2009 (1999).
  - [31] D. F. Walls and G. J. Milburn, *Quantum Optics* (Springer-

- Verlag, Berlin, 1994).
- [32] W. H. Press, B. P. Flannery, S. A. Teukolsky, and W. T. Vetterling, *Numerical Recipes* (Cambridge University Press, Cambridge, England, 1988).
- [33] H. M. Wiseman and G. J. Milburn, *Phys. Rev. Lett.* **70**, 548 (1993); K. Banaszek and K. Wódkiewicz, *ibid.* **76**, 4344 (1996); S. Wallentowitz and W. Vogel, *Phys. Rev. A* **53**, 4528 (1996).
- [34] S. Takeuchi, J. Kim, Y. Yamamoto, and H. H. Hogue, *Appl. Phys. Lett.* **74**, 1063 (1999).
- [35] C. Wu, J.-L. Chen, L. C. Kwek, and C. H. Oh, *Phys. Rev. A* **73**, 012310 (2006). In this very recent paper, the authors studied quantum nonlocality of  $N$ -qubit  $W$ -type entangled states, where a Bell violation for three-mode  $W$ -type single-photon entangled states,  $(|1,0,0\rangle+|0,1,0\rangle+|0,0,1\rangle)/\sqrt{3}$ , was not found using the parity measurements and the displacement operations. The author pointed out that this could be due to “displacement measurements” on the particles, which is in accordance with our understanding.
- [36] A. Cabello, *Phys. Rev. A* **65**, 032108 (2002).
- [37] L. V. Hau, S. E. Harris, Z. Dutton, and C. H. Behroozi, *Nature (London)* **397**, 594 (1999).
- [38] B. Yurke and D. Stoler, *Phys. Rev. Lett.* **57**, 13 (1986).
- [39] T. B. Pittman and J. D. Franson, *Phys. Rev. Lett.* **90**, 240401 (2003).
- [40] J. Fiurášek, L. Mišta, and R. Filip, *Phys. Rev. A* **67**, 022304 (2003); H. Jeong, Ph.D. thesis, Queen’s University, Belfast, UK, 2003; S. D. Barrett, P. Kok, K. Nemoto, R. G. Beausoleil, W. J. Munro, and T. P. Spiller, *Phys. Rev. A* **71**, 060302(R) (2005).
- [41] K. Nemoto and W. J. Munro *Phys. Rev. Lett.* **93**, 250502 (2004); W. J. Munro, K. Nemoto, and T. Spiller, *New J. Phys.* **7**, 137 (2005).